OPEN

# DZ-2384 has a superior preclinical profile to taxanes for the treatment of triple-negative breast cancer and is synergistic with anti-CTLA-4 immunotherapy

Cynthia Bernier[a,b,*], Ahmed Soliman[a,b,*], Michel Gravel[a,b], Matthew Dankner[b], Paul Savage[b], Kevin Petrecca[c], Morag Park[b], Peter M. Siegel[b], Gordon C. Shore[a,b] and Anne Roulston[a,b]

**Triple-negative breast cancer (TNBC) is typically aggressive, difficult to treat, and commonly metastasizes to the visceral organs and soft tissues, including the lungs and the brain. Taxanes represent the most effective and widely used therapeutic class in metastatic TNBC but possess limiting adverse effects that often result in a delay, reduction, or cessation of their use. DZ-2384 is a candidate microtubule-targeting agent with a distinct mechanism of action and strong activity in several preclinical cancer models, with reduced toxicities. DZ-2384 is highly effective in patient-derived taxane-sensitive and taxane-resistant xenograft models of TNBC at lower doses and over a wider range relative to paclitaxel. When comparing compound exposure at minimum effective doses relative to safe exposure levels, the therapeutic window for DZ-2384 is 14–32 compared with 2.0 and less than 2.8 for paclitaxel and docetaxel, respectively. DZ-2384 is effective at reducing brain metastatic lesions when used at maximum tolerated doses and is equivalent to paclitaxel. Drug distribution experiments indicate that DZ-2384 is taken up more efficiently by tumor tissue but at equivalent levels in the brain compared with paclitaxel. Selective DZ-2384 uptake by tumor tissue may in part account for its wider therapeutic window compared with taxanes. In view of the current clinical efforts to combine chemotherapy with immune checkpoint inhibitors, we demonstrate that DZ-2384 acts synergistically with anti-CTLA-4 immunotherapy in a syngeneic murine model. These results demonstrate that DZ-2384 has a superior pharmacologic profile over currently used taxanes and is a promising therapeutic agent for the treatment of metastatic TNBC.** ***Anti-Cancer Drugs*** **29:774–785 Copyright © 2018 The Author(s). Published by Wolters Kluwer Health, Inc.**

**Anti-Cancer Drugs** 2018, **29**:774–785

**Keywords: breast cancer, diazonamide, docetaxel, microtubule-targeting agent, paclitaxel**

[a]Laboratory for Therapeutic Development, [b]Department of Biochemistry, Rosalind and Morris Goodman Cancer Research Centre and [c]Department of Neurology and Neurosurgery, McGill University, Montréal, Quebec, Canada

Correspondence to Anne Roulston, PhD, Room 915C, 3655 Promenade Sir William Osler, Montreal, Canada, QC H3G 1Y6
Tel: +1 514 398 5226; fax: +1 514 398 7384; e-mail: anne.roulston@mcgill.ca

*Cynthia Bernier and Ahmed Soliman contributed equally to the writing of this article.

**Received** 31 December 2017 **Revised form accepted** 3 May 2018

## Introduction

Triple-negative breast cancer (TNBC) is characterized by the absence of estrogen, progesterone, and HER2 receptors and represents 10–14% of breast cancers [1]. TNBCs lack effective targeted therapies and are generally more aggressive than non-TNBC breast tumors, with higher rates of distant recurrence and decreased overall survival [2]. Owing to the lack of targeted therapeutics for TNBC, the neoadjuvant standard of care includes anthracyclines, cyclophosphamide, and taxanes, and although patients initially respond well to these treatments [3], metastatic relapse occurs typically within the first 3–5 years after diagnosis [4]. Common sites of metastases for TNBC are the lung and the brain [5]. Treatments for metastatic disease include additional chemotherapies such as antimetabolites, DNA damaging agents, and additional microtubule-targeting agents (e.g. vinorelbine, eribulin, or ixabepilone) [3]. Neurological and hematological toxicities are the principal and dose-limiting adverse effects encountered with microtubule-targeting agents. Peripheral neuropathy is the most frequently experienced adverse neurological effect followed by cranial neuropathy and other neuropathies that can affect the digestive system and lead to cognitive issues and depression [6]. Thus, there is a need for improved chemotherapies, including microtubule-targeting agents with lower toxicity profiles and improved efficacy.

There is a promising opportunity for microtubule-targeting agents in combination with checkpoint

Supplemental Digital Content is available for this article. Direct URL citations appear in the printed text and are provided in the HTML and PDF versions of this article on the journal's website, www.anti-cancerdrugs.com.



0959-4973 Copyright © 2018 The Author(s). Published by Wolters Kluwer Health, Inc. DOI: 10.1097/CAD.0000000000000653

inhibitor immunotherapies for multiple cancer indications. Accumulating evidence now suggests that chemotherapeutics such as paclitaxel and vinblastine can, in part, mediate anticancer activity through either direct or indirect activation of cytotoxic immune responses [7]. There is a clear correlation in TNBC between intratumoral immune responses and prognosis [8,9]. Recent phase I clinical trials in heavily pretreated patients with TNBC have shown encouraging results with anti-PD-1 [10] and anti-PD-L1 antibodies [11], the latter showing a positive correlation with CTLA-4 and T-helper type 1 gene expression [12]. Data from a recent phase II trial in patients with TNBC have demonstrated that adding pembrolizumab (anti-PD-1) to standard neoadjuvant therapy (paclitaxel followed by doxorubicin and cyclophosphamide) boosts the estimated pathological complete response rate from 20 to 60% [13], illustrating the potential of combining microtubule-targeting agents with immune checkpoint therapies.

DZ-2384 is a novel synthetic derivative of diazonamide A, a compound isolated from the marine organism *Diazona angulata* [14,15]. Early synthetic analogs of diazonamide A such as AB-5 had highly potent antitumor activity with minimal toxicity [16]. DZ-2384 is a refined and more potent preclinical candidate that has shown efficacy in models of colon, breast, and pancreatic cancers as well as in models of aggressive acute lymphocytic leukemia [17]. DZ-2384 functions by binding directly to tubulin dimers near the vinca alkaloid-binding site of tubulin. It has a distinct mechanism of action from other vinca-binding compounds in that it straightens the curvature of polymerizing microtubules and increases the frequency of microtubule rescue [17]. The result is strong inhibition of mitotic spindle formation but a less destabilizing effect on microtubules in nondividing cells including neurons, which may account in part for its enhanced safety margin. Retention of the microtubule network in cortical neurons at therapeutic doses of DZ-2384 may explain the lack of peripheral neuropathy at effective doses in preclinical models [17].

Here, we demonstrate the superior activity and therapeutic window of DZ-2384 compared with paclitaxel and docetaxel in several orthotopic patient-derived xenograft (PDX) and metastatic models of TNBC. DZ-2384 has superior activity over a wider dose range compared with paclitaxel in two PDX models from heavily pretreated patients with TNBC. To gauge DZ-2384 efficacy relative to toxicity, we measured compound exposure (area under the concentration time curve, AUC) at minimum effective doses to obtain a therapeutic window. The therapeutic window of DZ-2384 in the orthotopic PDX model and lung metastases model is 14 and 18.6, respectively. This compares favorably to the therapeutic windows of approximately two-fold for the taxanes paclitaxel and docetaxel. As promising results are emerging from clinical trials combining microtubule-targeting agents with immune checkpoint therapies, we demonstrate here that DZ-2384 synergizes with an anti-CTLA-4 therapy in a syngeneic model. The models selected in this study reflect the most robust and reproducible models in which to test the activity of DZ-2384 and do not necessarily reflect the eventual clinical path for the compound in humans. These results highlight the preclinical activity and safety margin of DZ-2384 in multiple TNBC models and indicate its potential use as a more efficacious and less toxic alternative to taxanes for metastatic TNBC.

## Materials and methods

### Compounds and formulations

DZ-2384 (synthesized as described in Ding *et al.* [18] by Paraza Pharma, Montreal, Quebec, Canada), docetaxel, and paclitaxel (LC Laboratories; Woburn, Massachusetts, USA) were prepared in DMSO and then diluted in cell culture media (DMSO 0.2% final) for evaluation *in vitro*. All three compounds were formulated in cremophor EL : ethanol : saline (5 : 5 : 90) (vehicle) for intravenous administration into animals.

### Cell lines and viability

MDA-MB-231, BT-549, MDA-MB-436, HCC1937, and RenCa cells are from ATCC (Manassas, Virginia, USA) and cultured according to the supplier's instructions. MDA-MB-231-LM2 [19] and MDA-MB-231-BrM2 [20] cells, selected for their ability to form lung and brain metastases, respectively, were obtained from Dr. Joan Massagué and cultured in Roswell Park Memorial Institute 1640 media supplemented with 10% fetal bovine serum, 2-mmol/l L-glutamine, 100 µg/ml streptomycin, and 10 U/ml penicillin. Cell lines were used within 10–15 passages of the vial of origin but were not further authenticated. Primary TNBC cells GCRC-1915 and GCRC-1735 were generated from dissociated patient-derived xenografts and were grown in Dulbecco's modified Eagle's medium (DMEM) supplemented with 10% fetal bovine serum, 2-mmol/l L-glutamine, 100 µg/ml streptomycin, and 10 U/ml penicillin. All cell lines were grown at 37°C in a humidified environment with 5% $CO_2$, with the exception of MDA-MB-436, which was grown without $CO_2$. Cell viability was determined in multiwell assay plates after 72 h of drug treatment using the CellTiter-Glo Luminescent Cell Viability Assay (Promega; Fitchburg, Wisconsin, USA) according to manufacturer's instructions. Sigmoidal dose–response curves were generated to calculate the concentration of drug resulting in 50% ($IC_{50}$) growth inhibition (Prism v6; GraphPad, La Jolla, California, USA). A cell line expressing Zs-Green-luciferase was derived from the GCRC-1945 PDX by infecting short-term (< 48 h) mammosphere cultures (DMEM/F12, 1× B27, 20 ng/ml human epidermal growth factor, 10 µg/ml insulin, 0.5 mg/ml hydrocortisone, 20 ng/ml basic fibroblast growth factor, 10 µg/ml heparin, 50 µg/ml gentamicin on ultra-low attachment plates) with pHIV-Luc-ZsGreen (Addgene; Cambridge, Massachusetts, USA) lentiviral particles.

### Animal studies

All animal experiments were performed in strict accordance with the Canadian Council on Animal Care and McGill University Animal Care committee guidelines. The maximum tolerated doses of DZ-2384, paclitaxel, and docetaxel were determined in four mice of the appropriate strain, which were administered compounds in four biweekly intravenous injections. For all experiments, monitoring of animal general condition was performed at least three times a week. Experimental end points were determined to be body weight lost higher than 20% for more than three consecutive days, mouse survival, or severe signs of distress. Animal weights, clinical signs, and survival were recorded until 1 week after the last dose of compound. Primary PDXs were established from primary tumor tissue obtained at the time of surgery from patients as part of the McGill University Hospital Centre Breast Cancer Functional Genomics Initiative. Tumor fragments (1–1.5 $mm^3$ cubes) from GCRC-1945 and GCRC-2076 were implanted and expanded into the left fat pad of female NOD.Cg-Prkdc$^{scid}$Il2rg$^{tm1Wjl}$/SzJ (NSG) mice (6–8 weeks old; Jackson Laboratories) and were propagated for not more than eight passages. Tumor diameters were measured with digital calipers, and the tumor volume was estimated using the following: volume ($mm^3$) $= 4/3\pi$ $[(a/2)\times(b/2)^2]$, where '$a$' and '$b$' are the largest and smallest diameters, respectively, of the tumor. Animals were randomized when tumors reached 100–250 $mm^3$. PDX models were treated with vehicle, DZ-2384, or paclitaxel intravenously once weekly for 4 weeks. In the lung metastases model, female CB17.Cg-Prkdc$_{scid}$Lyst$_{bg\text{-}J}$/Crl (SCID-beige) (6–8 weeks old; Charles River, Wilmington, Massachusetts, USA) mice were injected with $2.5\times10^5$ MDA-MB-231-LM2 cells into the lateral tail vein. Lung metastases were monitored by bioluminescent imaging, and mice were randomized into treatment groups according to tumor burden before receiving four biweekly intravenous injections of vehicle, DZ-2384, or docetaxel. In the brain metastatic tumor model, either MDA-MB-231-BrM2 ($7.5\times10^4$ cells) or GCRC-1945 expressing luciferase pHIV-Zs-Green-Luciferase ($1\times10^5$ cells) was implanted intracranially into the right frontal lobe of NSG mice (female, 6–8 weeks, NSG; Jackson Laboratories, Bra Harbor, Maine, USA) under sterile surgical conditions as described in the study by Donoghue *et al.* [21]. Mice were randomized according to tumor burden derived from bioluminescent imaging values and then treated with vehicle, DZ-2384, or paclitaxel (intravenously; biweekly for 2 weeks). The efficacy of the DZ-2384 and CTLA-4 combination was evaluated in the RenCa mouse renal carcinoma model by injecting cells ($2.5\times10^5$) into the left lower flank of Balb/c mice (6–8 weeks; Charles River). Mice were randomized into groups when the average tumor size reached 100–150 $mm^3$. Animals received a single intravenous injection of vehicle or DZ-2384 (14 mg/kg) on day 1 and were subsequently treated with four biweekly intraperitoneal injections of CTLA-4 antibody (Clone: 9H10; Bio X Cell Inc., Lebanon, New Hampshire, USA) or Rat IgG2a isotype control (Clone: 2A3; Bio X Cell Inc.). In all efficacy experiments, body weight and tumor sizes were measured two-three times a week, whereas tumor imaging was performed once weekly.

### In-vivo bioluminescent imaging and analysis

Bioluminescence imaging was carried out using the IVIS animal imaging system (Caliper Life Biosciences, Hopkinton, Massachusetts, USA) and analyzed using Living Image software. Ten minutes before imaging, mice were injected intraperitoneally with XenoLight D-Luciferin-$K^+$ Salt Substrate (Perkin Elmer; Waltham, Massachusetts, USA) at 150 mg/kg. Mice were then anesthetized and imaged over a 1-min interval for 7–8 min. Using the Living Image software (Perkin Elmer), signal intensity was quantified within a defined region of the mouse and then the flux of photon counts quantified.

### Pharmacokinetics

To measure compound exposure levels to DZ-2384 and docetaxel in female SCID-beige mice ($AUC_{0-\infty}$), compounds were administered intravenously as a single dose ($n=4$) at the minimum effective doses of 0.5 and 4 mg/kg, respectively. Blood samples were microsampled at 0, 0.08, 0.25, 0.5, 1, 2, 4, 8, and 24 h for each mouse, and then the plasma was isolated and snap frozen on dry ice before quantification by liquid chromatography–mass spectrometry (LC–MS/MS) (see below). To measure the tissue distribution of DZ-2384 and paclitaxel at the maximum tolerated dose in plasma, brain, heart, lung, and tumor tissue in female NSG mice ($AUC_{0-\infty}$), DZ-2384 (10 mg/kg) and paclitaxel (40 mg/kg) were administered intravenously as a single dose ($n=4$) per time point, and plasma was collected at 0, 0.5, 1, 2, 4, 8, and 24 h. At the indicated time points, the animals were rapidly perfused with a 20-ml injection of saline into the left cardiac ventricle before tissue harvest to remove blood from the tissue. To measure compound exposure levels to DZ-2384 and paclitaxel in female NSG mice ($AUC_{0-\infty}$), compounds were administered intravenously as a single dose ($n=4$) at the minimum effective doses of 1.25 and 10 mg/kg, respectively. Blood samples were microsampled at 0, 0.08, 0.25, 0.5, 1, 2, 4, 8, and 24 h for each mouse and plasma isolated. All plasma and tissue samples were snap frozen on dry ice before quantification by LC–MS/MS. PK parameters were calculated using Kinetica Software (ThermoFisher Scientific; Waltham, Massachusetts, USA) for pharmacokinetic/pharmacodynamic data analysis. Results represent the mean values for four mice per dose group.

### Compound extraction and quantification by LC–MS/MS

DZ-2384 and paclitaxel were extracted from plasma with 2.5 volumes of acetonitrile : methanol (80 : 20) containing the internal standard DZ-2362. To extract drugs from tissues, a volume of 25% acetonitrile in water equal to

five times the weight of each tissue was added before homogenization in two volumes of acetonitrile : methanol (80 : 20). After vortexing, and centrifugation for 15 min at 3500 rpm, 4°C, supernatant from both plasma and tissue extracts were transferred into an HPLC plate, and two volumes of water + 0.1% formic acid were added. DZ-2384-containing samples were analyzed in MRM mode by LC–MS/MS (AB/SCIEX 4000 QTRAP, Agilent 1100 series high-performance liquid chromatography system, Santa Clara, California, USA) using a Luna C8(2), 30 × 2 mm, 5 µmol/l column, and a flow rate of 0.70 ml/min. Mobile phase was A: $H_2O$ + 0.1% formic acid and B: 20/80 isopropanol/acetonitrile + 0.1% formic acid, with a gradient of 10–98% B in 1.5 min, plateau at 98% B for 1.9 min; docetaxel-containing and paclitaxel-containing samples were analyzed in the same way but with mobile phase A: $H_2O$ + 0.1% formic acid and 5 mmol/l $NH_4$ formate, pH 4.5, and B: 95/5 methanol /H2O + 5 mmol/l $NH_4$ formate + 0.5 mmol/l Na formate with a gradient of 20–100% B in 1.5 min, plateau at 100% B for 1.4 min; paclitaxel was quantified relative to standard curves.

## Results

### TNBC cell line sensitivity to DZ-2384

To investigate the potential activity of DZ-2384 in the TNBC setting, we initially evaluated the potency of the compound in a panel of TNBC cell lines including two recently derived from primary TNBC tumor explants. DZ-2384 was as potent as paclitaxel and docetaxel ($IC_{50}$s at low nmol/l levels) in all cell lines tested with the exception of HCC1937, which was cross-resistant to DZ-2384, paclitaxel, and docetaxel (Table 1). Given that HCC1937 overexpresses the ABCG2 multidrug resistant pump [22] and is also resistant to doxorubicin [23] and olaparib [24], it is possible that DZ-2384 is also susceptible to multidrug resistant mechanisms. These data demonstrate that DZ-2384 is highly potent across a range of TNBC cell lines with varied genetic aberrations and molecular classifications.

### Efficacy of DZ-2384 in PDX and metastatic models of TNBC

PDX models more closely recapitulate human tumor characteristics than cell line-derived models with respect to tissue histology, tumor heterogeneity, mRNA or protein expression profiles, and metastatic behavior [25]. To investigate the efficacy of DZ-2384 *in vivo*, we selected two PDX models: GCRC-1945 and GCRC-2076. The tumor tissue from both PDXs was derived from metastases of patients previously treated with doxorubicin, cyclophosphamide, carboplatin, and paclitaxel. In addition, patient GCRC-1945 received capecitabine and is taxane sensitive as a PDX model, whereas patient GCRC-2076 received methotrexate and 5-fluorouracil and is more taxane resistant. To equilibrate the experimental doses relative to toxicity, DZ-2384 and paclitaxel dose levels were selected as a function of their respective maximum tolerated doses (MTD) in nontumor bearing NSG mice (10 and 40 mg/kg, respectively). The MTD was defined as the maximum dose (administered biweekly for 2 weeks) that does not cause any lethality, leads to less than 20% body weight loss, and causes no unacceptable clinical effects (Supplementary Fig. 1, Supplemental digital content 1, *http://links.lww.com/ACD/A262*). The PDX tumor tissue was implanted into the mammary fat pad of NSG mice and antitumor activity monitored by measuring tumor volume and survival (Fig. 1). The results demonstrate that at 0.125× and 0.25× MTD, DZ-2384 is more effective than paclitaxel in the GCRC-1945 model resulting in tumor regression and increased median survival. However, at 0.5× MTD, DZ-2384 and paclitaxel were equally effective (Fig. 1a and b). We define the minimum effective dose (MED) as the minimum dose required to cause a statistically significant tumor regression. In the GCRC-1945 model, the MED for DZ-2384 was 1.25 mg/kg (0.125× MTD) and increased median survival from 36 to 71 days, whereas the MED for paclitaxel was 10 mg/kg (0.25× MTD) and increased median survival up to 53 days. In the GCRC-2076 paclitaxel-resistant model, the DZ-2384 was more effective than paclitaxel at 0.25× and 0.5× MTD, and paclitaxel was not effective at 0.25× MTD (Fig. 1c and d). In this model at 0.5× MTD doses for DZ-2384 and paclitaxel, the median survival was increased from 30 days to 88 and 69 days, respectively. These data suggest that at lower doses, DZ-2384 has superior efficacy than paclitaxel and is effective over a wider dose range. Treatment with DZ-2384 could therefore be highly effective in paclitaxel-resistant tumors.

**Table 1** The in-vitro sensitivity of triple-negative breast cancer cell lines to DZ-2384, paclitaxel, and docetaxel

| | | | | $IC_{50}$ (nmol) | | |
|---|---|---|---|---|---|---|
| Cell lines | Pathology | Molecular classification | Genetic aberrations | DZ-2384 | Paclitaxel | Docetaxel |
| MDA-MB-231 | AC | Basal B | P53 (mt), KRas (mt) | 7.7 | 6.0 | 2.2 |
| MDA-MB-436 | IDC | Basal B | P53 (mt), BRCA1 (homo mt) | 2.8 | 9.9 | 3.7 |
| BT-549 | IDC | Basal B | P53 (mt), PTEN homo deletion | 0.66 | 3.1 | 1.0 |
| HCC1937 | IDC | Basal A | P53 (mt), BRCA1 (homo mt), PTEN homo deletion | > 2500 | > 2500 | > 2500 |
| GCRC-1915 | IDC | Basal | unknown | 17 | 5.0 | 3.7 |
| GCRC-1735 | IDC | Basal | BRCA1 (mt) P53 (mt) | 7.0 | 1.9 | 3.7 |

AC, adenocarcinoma; IDC, invasive ductal carcinoma.

**Fig. 1**

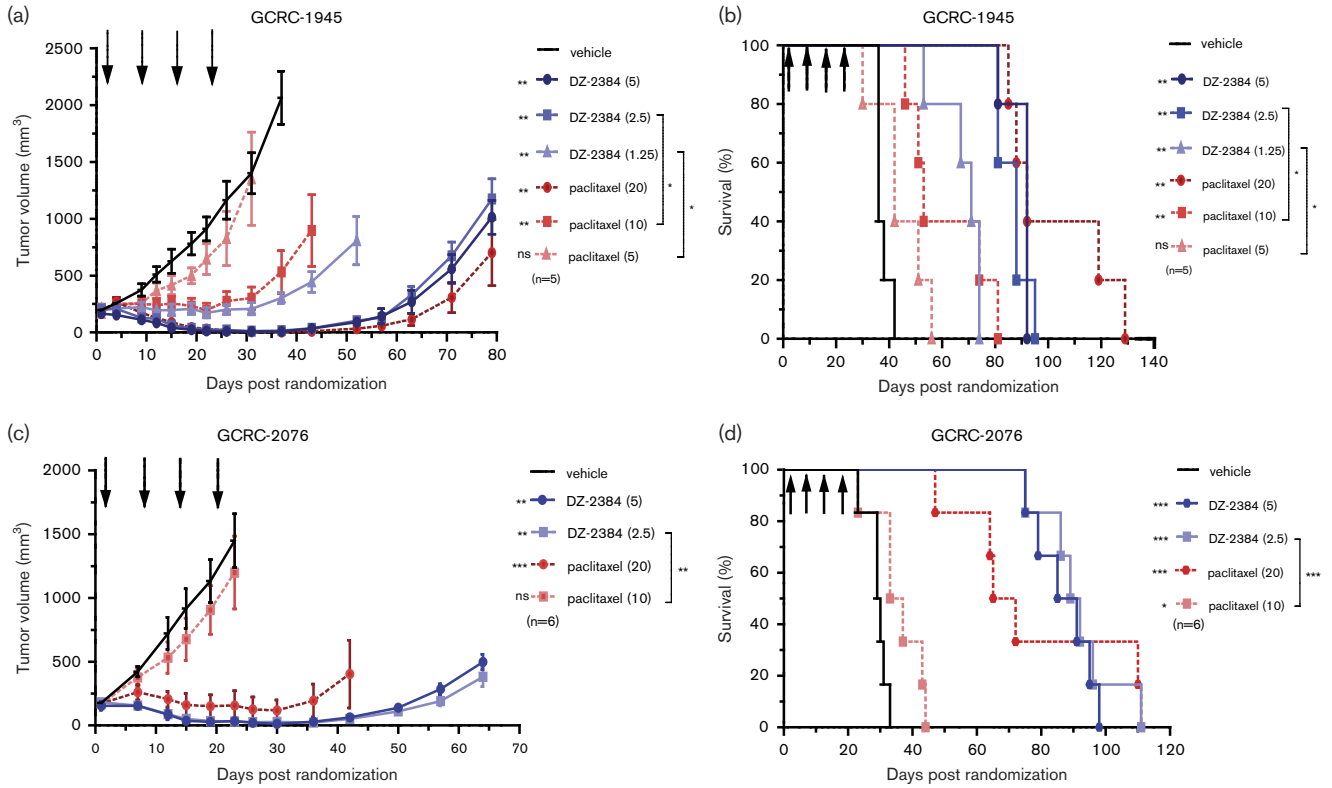


Antitumor activity of DZ-2384 and paclitaxel in triple-negative breast cancer (TNBC) patient-derived xenograft (PDX) GCRC-1945 and GCRC-2076 models. Mice implanted with PDXs in the mammary fat pad (a, b) GCRC-1945 or (c, d) GCRC-2076 tumors were treated four times weekly with DZ-2384 or paclitaxel (indicated by black arrows at the dose shown in mg/kg in brackets in the legend). (a, c) Data represent mean tumor volume ± SEM. Asterisks on the left of the legend represent statistical differences with vehicle control, asterisks on the right represent statistical differences between groups according to Student's *t*-test. (b, d) Kaplan–Meier curves represent animal survival. Statistical significance was determined by log-rank (Mantel–Cox) test relative to vehicle-treated animals. Asterisks on the left of the legend represent differences with vehicle control, on the right differences between groups. $^{*}P < 0.05$, $^{**}P < 0.005$, $^{***}P < 0.0001$.

The major sites of metastases for TNBC are the lung/pleura followed by bone, liver, and brain [26–28]. As a representative model of visceral metastases, we selected the MDA-MB-231-LM2 lung metastatic model. This TNBC xenograft model selectively develops lung metastases and stably expresses luciferase such that tumor growth can be monitored by bioluminescent imaging [19]. In this model, the efficacy of DZ-2384 was compared with docetaxel, a newer taxane used commonly in (first, second, and third lines) the treatment of metastatic TNBC. MDA-MB-231-LM2 cells were injected by tail vein into SCID-beige mice, and ~2 weeks later, animals with confirmed lung metastases were randomized into treatment groups. DZ-2384 treatment resulted in a profound antitumor effect at all doses tested, and at 4.5 mg/kg, the median survival increased from 37 to more than 150 days (Fig. 2a and b), and at 5 months after treatment initiation, four of nine mice were tumor free (determined by bioimaging). Docetaxel was effective at only the 4 mg/kg dose and did not result in the survival of any mice beyond 3 months following treatment initiation (Fig. 2c and d). The MED for DZ-2384, as demonstrated by a reduction in tumor volume and by increased survival, was 0.5 mg/kg, whereas the MED for docetaxel was 4 mg/kg. At these doses, more than 10% weight loss is observed only for 4 mg/kg docetaxel (Supplementary Fig. 2, Supplemental digital content 1, *http://links.lww.com/ACD/A262*). The MTDs of DZ-2384 and docetaxel are 12 and 4 mg/kg, respectively. This, in contrast to docetaxel, highlights the efficacy of DZ-2384 at doses well below the MTD. These results for DZ-2384, in a difficult-to-treat lung metastatic model, are consistent with its improved efficacy in PDX models, demonstrating that it is effective over a wider dose range compared with docetaxel.

Metastases to the brain occur more frequently in TNBC than in luminal-type breast cancers [26] and are difficult to treat, as many chemotherapeutics do not cross the blood–brain barrier [29]. To compare the efficacy of DZ-2384 with taxanes in a brain metastastic model, brain tropic TNBC MDA-MB-231-BrM2 [20] and PDX GCRC-1945 cells were engineered to stably express luciferase

**Fig. 2**

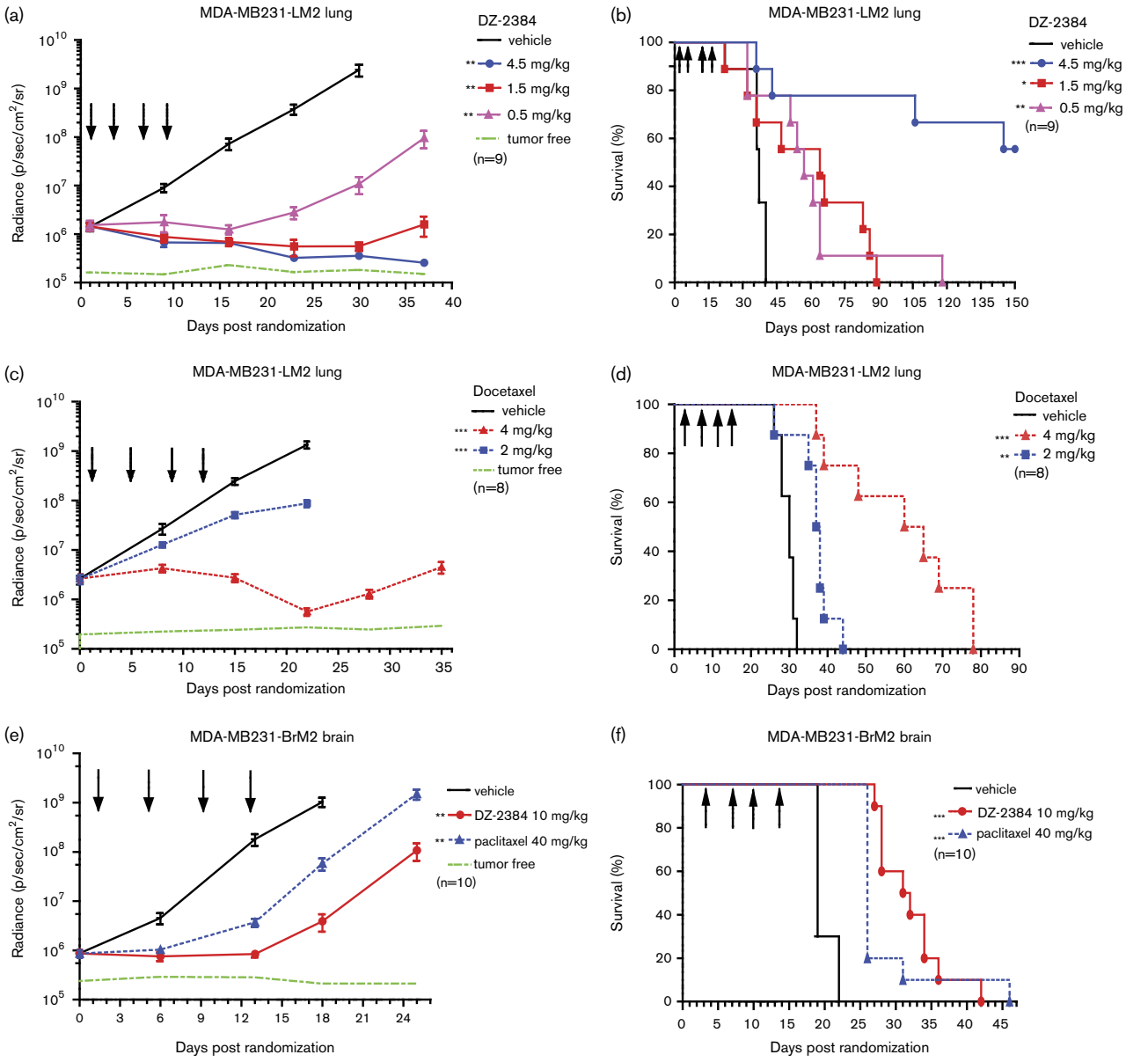


Antitumor activity of DZ-2384, docetaxel, and paclitaxel in metastatic lung and brain triple-negative breast cancer (TNBC) models. (a–d) Mice bearing MDA-MB-231-LM2 lung metastases were treated biweekly for 2 weeks with DZ-2384 (a, b) or docetaxel (c, d) biweekly for 2 weeks (treatment days indicated by arrows). (e, f) Mice bearing intracranially transplanted MDA-MB-231-BrM2 cells were treated biweekly for 2 weeks with DZ-2384 or paclitaxel (treatment days indicated by arrows). (a, c, e) Mean bioluminescence signal ± SEM measured weekly. A tumor-free animal was imaged to represent the background signal. (b, d, f) are Kaplan–Meier curves depicting survival. Statistical differences with vehicle control are indicated to the left of the legend and were determined by Student's *t*-test for bioluminescence and log-rank (Mantel–Cox) test for survival curves. Asterisks on the left of the legend represent differences with vehicle control, on the right differences between groups. $^{*}P < 0.05$, $^{**}P < 0.005$, $^{***}P < 0.0001$.

such that the tumor burden could be monitored by luminescence bioimaging. To simulate brain metastases, while minimizing disruption to the blood–brain barrier, tumor cells were injected intracranially in the right frontal lobe and allowed to grow until a sufficient brain tumor signal was detected. Animals randomized according to tumor burden were then treated at doses representing the MTD of DZ-2384 or paclitaxel. The results demonstrate that DZ-2384 is efficacious in both MDA-MB-231-BrM2 (Fig. 2e and f) and GCRC-1945 models (Supplementary Fig. 3A and B, Supplemental digital content 1, *http://links.lww.com/ACD/A262*), decreasing tumor burden and increasing the median survival relative to vehicle control-treated animals. In comparison with paclitaxel in both models, there is significant improved efficacy with DZ-2384 in tumor burden but not survival. The body weight

loss experienced by mice treated with either agent was less than 10% (Supplementary Fig. 3C and D, Supplemental digital content 1, *http://links.lww.com/ACD/A262*).

### The therapeutic window of DZ-2384 compared with taxanes

DZ-2384 is more effective at lower doses in xenograft models compared with paclitaxel and docetaxel; however, the true therapeutic window relates compound exposure at effective levels (the MED) to exposure at safe and tolerated levels. The exposure levels of compound at minimum effective levels were compared with those in patients receiving paclitaxel and docetaxel at clinical doses for TNBC (Table 2). Typically, the dose established in clinical trials represents the maximum tolerated dose in humans. Paclitaxel exposure at the MED in the GCRC-1945 PDX model is only two-fold lower than exposure in patients (15 797 ng h/ml) at clinically approved doses (175 mg/m$^2$) for TNBC [30]. Similarly, docetaxel exposure at MED in the MDA-MB-231-LM2 model is 1.7-fold lower than exposure (4810–5200 ng h/ml) in patients receiving a 100 mg/m$^2$ dose for TNBC [31,32].

The most significant dose-limiting toxicities of the taxanes are neutropenia and peripheral neuropathy, which often leads to treatment discontinuation or dose reduction, resulting in a less effective treatment course for patients. Previously, the effects of DZ-2384 and docetaxel were evaluated in a rat model of peripheral neuropathy [17]. DZ-2384 had no detrimental effects on peripheral nerves at effective levels. To determine the therapeutic window relative to peripheral neuropathy, DZ-2384 and docetaxel exposures at the MED in the MDA-MB-231-LM2 lung metastases model were related to the exposure at the maximum non-neurotoxic dose in the rat neuropathy study (Table 2). The lowest dose of docetaxel tested (10 mg/kg) in the rat peripheral neuropathy study resulted in mild neuropathy characterized by a 12–23% loss in digital and caudal nerve conduction velocity [17]. We therefore assume that this value is above the maximum non-neurotoxic dose and leads to an overestimation of therapeutic window for docetaxel. The therapeutic window of DZ-2384 relative to neurotoxicity is 18.6 compared with less than 2.8 for docetaxel in the MDA-MB-231-LM2 model. Importantly, a DZ-2384 plasma exposure of 8398 ng h/ml in mice represents a level at which no adverse effects on blood cell counts, biochemistry, and bone marrow occurred [17]. Relating this level to effective levels for DZ-2384 in the GCRC-1945 and MDA-MB-231-LM2 models represents a therapeutic window of 26.9- and 32.3-fold, respectively. These results illustrate that DZ-2384 has substantially wider safety margin than both paclitaxel and docetaxel.

### DZ-2384 distribution to brain and tumor tissue

The mechanistic principle behind the high therapeutic window of DZ-2384 is its distinct effect on microtubule dynamics and its unique ability to preserve the microtubule infrastructure in nondividing cells including neurons [17]. To further understand the distribution of DZ-2384 and its concentration within tissues at its site of action, we explored the tumor, brain, and tissue distribution in comparison with paclitaxel. Animals bearing MDA-MB-231-BrM2 tumors implanted into the mammary fat pad were used for these experiments. The animals did not have any brain metastases at the time of the experiment, as verified by bioluminescent imaging, indicating that the blood–brain barrier was likely not compromised. DZ-2384 and paclitaxel were administered to animals, and then plasma and tumor, lung, brain and heart tissues were sampled over time up to 24 h. The proportions of DZ-2384 and paclitaxel that accumulate in the brain relative to plasma exposure are 15 and 12%, respectively (Fig. 3a and b). These results are consistent with previously published brain/plasma paclitaxel proportions [33,34]. The DZ-2384 and paclitaxel distributions in the lung and heart are very close to levels in the plasma; furthermore, the distribution in these tissues is also equivalent between DZ-2384 and paclitaxel. Interestingly, DZ-2384 has an 18-fold accumulation in tumor tissue relative to plasma, a level that is six times

**Table 2** The therapeutic window of DZ-2384 relative to paclitaxel and docetaxel

| Compounds | MED in PDX GCRC-1945 (mg/kg) | MED in MDA-MB-231-LM2 (mg/kg) | Minimum effective exposure level $AUC_{0-\infty}$ (ng h/ml) | Safe exposure level AUC (ng h/ml) | Therapeutic window (minimum effective vs. safe exposure levels) |
|---|---|---|---|---|---|
| Paclitaxel | 10 | – | 7830 | 15 797[a] | 2.0 |
| Docetaxel | – | 4 | 2896 | 5005[b] | 1.7 |
| | | | | 8113[c] | < 2.8 |
| DZ-2384 | 1.25 | – | 312 | 4371[d] | 14.0 |
| | – | 0.5 | 235 | | 18.6 |
| | 1.25 | – | 312 | 8398[e] | 26.9 |
| | – | 0.5 | 235 | | 32.3 |

AUC, area under the curve; MED, minimum effective dose.
[a]Human exposure: paclitaxel AUC at clinical dose of 175 mg/m$^2$ [26].
[b]Human exposure: mean docetaxel AUC at clinical dose of 100 mg/m$^2$ [27,28].
[c]Lowest dose tested in rat neurotoxicology study. Dose at which there is ~ 20% body weight loss, 12–23% loss in digital and caudal nerve conduction velocity suggesting some peripheral neuropathy [17].
[d]Maximum non-neurotoxic dose determined in a rat neurotoxicology study [17].
[e]No observable adverse effect level. Dose at which no clinical signs or adverse effects on blood biochemistry, hematology, and bone marrow were observed [17].

**Fig. 3**

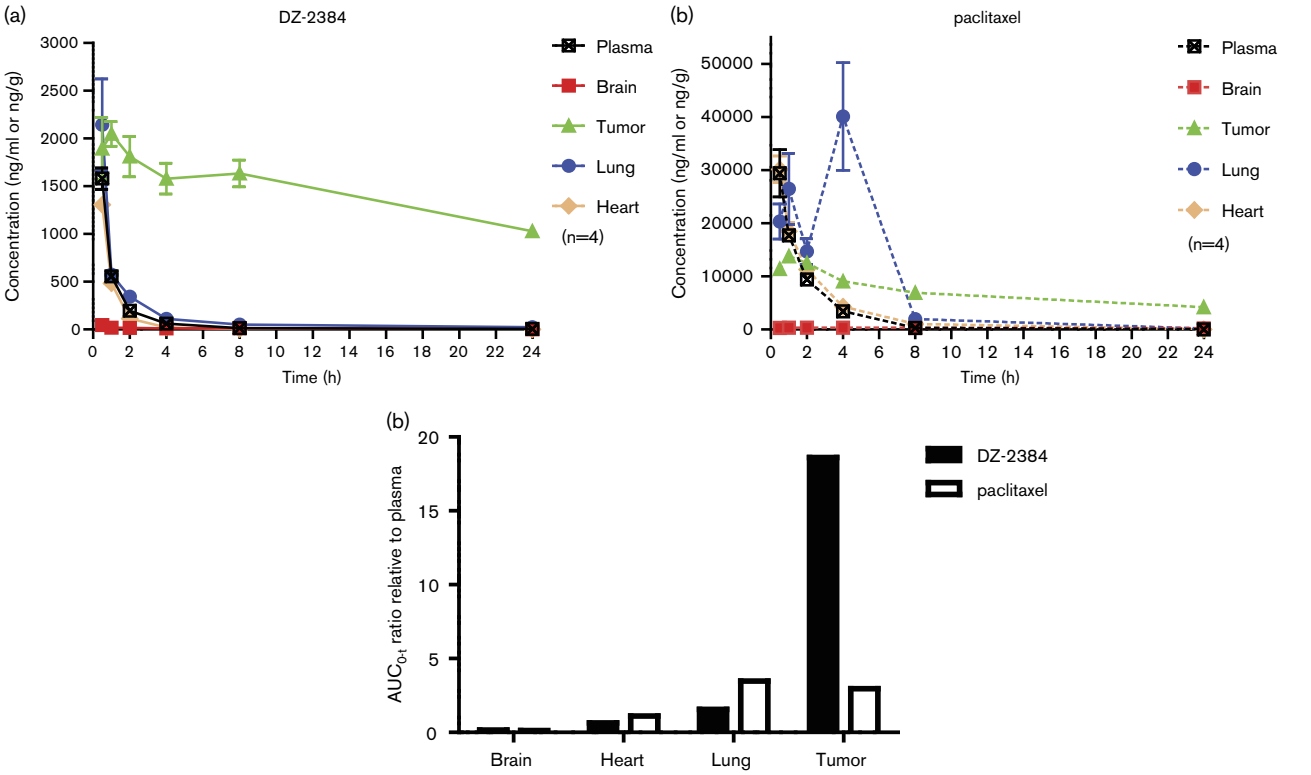


The pharmacokinetic profile of DZ-2384 and paclitaxel in plasma, brain, tumor, lung, and heart. NSG mice ($n = 4$/time point) were administered (a) DZ-2384 (10 mg/kg) or (b) paclitaxel (40 mg/kg) intravenous bolus in a Cre : EtOH : saline (5 : 5 : 90) vehicle. At the indicated time points, blood was taken for plasma isolation, and the animals perfused with saline before isolation of the brain, lung, heart and tumor tissues resected from the mammary fat pad. DZ-2384 and paclitaxel were quantified in each tissue by LC–MS/MS, and the mean ± SEM are presented. (c) The exposure ($AUC_{0-\infty}$) ratio of DZ-2384 (black bars) and paclitaxel (white bars) in the brain, heart, lung and tumor tissue relative to plasma. AUC, area under the curve; LC–MS/MS, liquid chromatography–mass spectrometry.

higher than for paclitaxel (Fig. 3c). The pharmacokinetic profile of DZ-2384 in the tumor compared with plasma suggests that there is both increased uptake and retention of drug in the tumor tissue (Supplementary Table 1, Supplemental digital content 1, *http://links.lww.com/ACD/A262*). The uptake is represented by a maximum concentration ($C_{max}$) ratio in tumor relative to plasma of 1.3 for DZ-2384 compared with 0.47 for paclitaxel. Retention is represented by the $t_{1/2}$ and is 29.3 h for DZ-2384 compared with 19.1 h for paclitaxel. These results demonstrate the selective accumulation of DZ-2384 in tumor tissue and provide an additional pharmacokinetic explanation for the higher therapeutic window of DZ-2384 relative to paclitaxel.

### The efficacy of DZ-2384 in combination with immune checkpoint inhibitors

Accumulating evidence now suggests that chemotherapeutics such as paclitaxel and vinblastine can in part mediate anticancer activity through either direct or indirect modulation of cytotoxic immune responses [7] and a clear correlation exists in TNBC and in other tumor types between intratumoral immune responses and prognosis [8,9]. In this context, we sought to evaluate the possibility that DZ-2384 would enhance the activity of immune checkpoint inhibitor therapy. We selected the RenCa renal syngeneic model in which to test this hypothesis, as it is a reliable and sensitive model in which to test murine surrogate anti-CTLA-4 antibody therapy [35]. Previous experimental results obtained in animal models and humans suggest that optimum synergy between two treatments is obtained when the immunotherapy is administered shortly after chemotherapy [36]. Animals bearing RenCa tumors were treated with a single dose of DZ-2384 followed 4 days later by biweekly treatments with anti-murine CTLA-4 antibody for 2 weeks (Fig. 4). Although DZ-2384 (single dose) and anti-CTLA-4 treatments alone had modest effects on tumor volume relative to vehicle control within the first 18 days of treatment, the combination of DZ-2384 and anti-CTLA-4 synergistically enhanced the antitumor effect and resulted in complete tumor regression in six of seven mice (Fig. 4a–d). Anti-CTLA-4 as a single agent enhanced the median survival of treated animals from 21 to 43 days, and the combination of DZ-2384 before anti-CTLA-4 resulted in the long-term survival of six of seven

**Fig. 4**

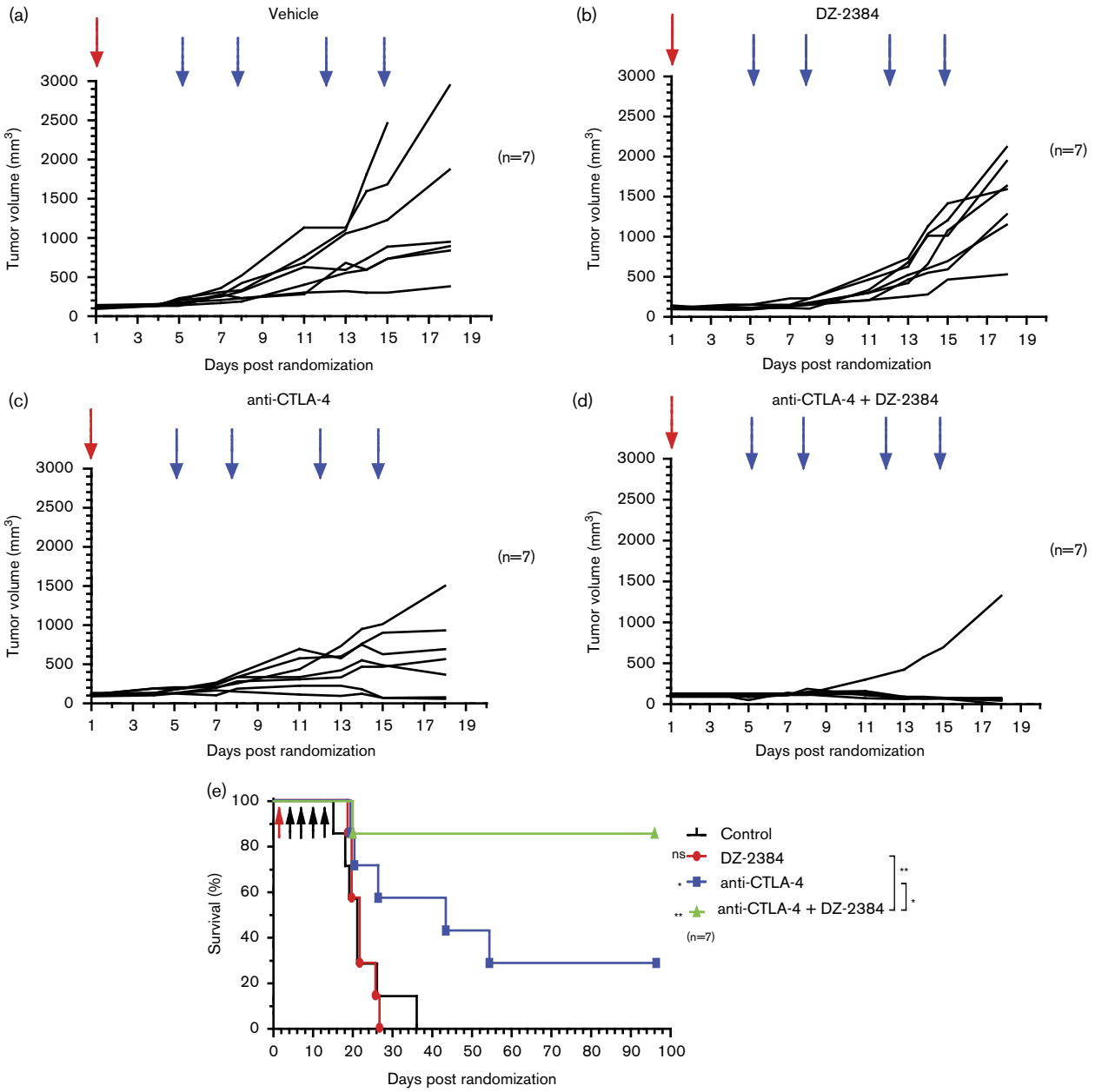


The efficacy of the DZ-2384 and anti-CTLA-4 combination in the RenCa syngeneic model. Balb/c mice bearing RenCa tumors ($n = 7$) were treated with (a) vehicle, (b) DZ-2384, (c) anti-CTLA-4, and (d) DZ-2384 + anti-CTLA-4. Each group was treated once with either DZ-2384 at 14 mg/kg or vehicle (solid arrow) on day 1 and then either anti-CTLA-4 antibody or Rat IgG2a isotype control, at 10 mg/kg (dotted arrows), on biweekly for 2 weeks. The DZ-2384 vehicle is Cre : EtOH : saline (5 : 5 : 90). (a–d) Tumor volumes of each mouse ($n = 7$). (e) A Kaplan–Meier curve depicting survival. Asterisks on the left of the legend represent differences with vehicle control, on the right differences between groups.*$P < 0.05$,**$P < 0.005$.

animals (82 days after treatment completion) (Fig. 4e). This demonstrates that DZ-2384 has the potential to significantly boost immune checkpoint inhibitor therapies, a strategy that could be widely applicable to many tumor types where immunotherapies are used. Together, these results support further development of DZ-2384 for the treatment of metastatic TNBC as a single agent or in addition to immune checkpoint inhibitors.

## Discussion

Despite the clinical success of microtubule-targeting agents such as taxanes in metastatic TNBC, a substantial proportion of patients experience unacceptable toxicities without the benefit of long-term survival. Here, we highlight the superior therapeutic window of DZ-2384 relative to two taxanes by establishing the minimum effective exposure level in TNBC PDX and lung metastases

models. Taxane exposure at minimum effective doses compared with exposure at a safely established clinical dose represents an approximate two-fold therapeutic window for paclitaxel and docetaxel. This is similar to the therapeutic window estimated for docetaxel (< 2.8) based on MDA-MB-231-LM2 model efficacy compared with peripheral neuropathy in the rat model. However, using the same comparison, we find that DZ-2384 is effective at exposure levels of 14.0- and 18.6-fold below the maximum non-neurotoxic level. Similarly, the DZ-2384 minimum effective levels are 26.9- and 32.3-fold below levels that show no adverse effects on blood biochemistry, hematology, and bone marrow toxicity. This indicates a substantial therapeutic window for DZ-2384 in contrast to the taxanes, with the potential to support dose reductions from MTD while retaining therapeutic activity. This important characteristic may prove particularly relevant to combinations of the agent with a variety of therapeutics, including immune-mediated therapies.

The inefficient brain uptake of the taxanes and the vinca alkaloids has been a limiting factor in the treatment of brain metastases from patients with metastatic TNBC [37]. Here, we find that DZ-2384 has a clear antitumor effect and increased survival compared with vehicle control in two different brain metastatic models. Compared with paclitaxel, there is an enhanced improvement in tumor burden but not in animal survival. The uptake of the two compounds is equivalent in animals without compromise to the blood–brain barrier. This suggests that the increase in activity for DZ-2384 relative to paclitaxel may result from its preferential cancer cell uptake. As brain metastases are known to enhance permeability of the blood–brain barrier [38], the 15% DZ-2384 brain uptake measured here would represent a minimum level of drug exposure to brain tumor tissue. DZ-2384 levels in the brain could potentially be enhanced by increased brain permeability in patients and by selective tumor uptake and therefore could affect brain metastases.

Tumor distribution experiments show that both paclitaxel and in particular DZ-2384 are preferentially taken up and retained in the tumor tissue. DZ-2384 has properties that allow for a tumor accumulation six times greater than for paclitaxel. The reason for the tumor accumulation of DZ-2384 compared with paclitaxel has not been investigated. However, the phenomenon of increased drug uptake and retention in solid tumor tissue has been attributed to various physical, chemical and pharmacokinetic properties of anticancer compounds and of the tumor microenvironment. Because of the enhanced metabolic activity and glycolysis in the actively dividing tumor, increased lactic acid is produced and accumulates in the extracellular matrix. These effects lead to pH differentials between tumor (including breast cancer) and normal tissue [39]. Extracellular pH can influence the cellular uptake and activity of various chemotherapeutics including anthracyclines, methotrexate, and chlorambucil [40]. Expression of the multidrug resistant pump, MDR1, can either positively or negatively influence drug uptake into tissue [41] by influencing drug penetration through multiple cellular layers. Some drugs such as the DNA intercalating anthracyclines accumulate in tumor tissue by binding to their target [42]. Likewise, DZ-2384 may be more readily bound to tubulin that is rapidly polymerizing and depolymerizing in dividing cells or DZ-2384 may have a higher affinity for human tubulin than for mouse tubulin, which could account for increased tumor uptake and retention in the xenograft tumor model.

Although TNBC is not considered a highly immunogenic tumor type, a clear correlation exists between intratumoral immune responses and overall prognosis [8,9,43]. There is evidence that immune evasion plays a role in TNBC tumor development and growth. TNBC has higher levels of immune checkpoint ligand and receptor expression relative to other breast cancer subtypes [44,45]; however, intervention with immune response checkpoints does not cause complete tumor responses in all patients. Early clinical trials with single agent immune checkpoint inhibitors targeting PD-1 and PD-L1 have indicated overall response rates of up to 19% in metastatic breast cancer despite the selection of patients whose tumors were PD-L1 positive [10,46].

Accumulating evidence indicates that many chemotherapies including microtubule-targeting agents have immune modulatory as well as direct cytotoxic effects on tumors [43,47]. One study in tumors from patients with TNBC showed that previous taxane therapy correlated with high mRNA expression of immune checkpoint genes including *PD-1*, *PD-L1*, and *CTLA-4* [48], providing a clear rationale for combining microtubule-targeting agents and immune checkpoint inhibitor therapies. Our results demonstrate a clear synergy between DZ-2384 and a murine anti-CTLA-4 checkpoint inhibitor that results in tumor size reduction and increased survival over administration of each alone. This occurs with a treatment schedule that includes an initial dose of DZ-2384 followed 4 days by biweekly doses of an anti-CTLA-4 checkpoint inhibitor for 2 weeks. Initial treatment with chemotherapy could provide a stimulatory effect on the immune system that boosts tumor antigen presentation and intratumoral inflammation. For example, paclitaxel causes macrophages to secrete inflammatory cytokines such as tumor necrosis factor-α, interleukins, and nitric oxide synthases in the tumor microenvironment that stimulate other immune and antigen-presenting cells such dendritic cells, natural killer cells, and cytotoxic T lymphocytes (reviewed in [47]). Paclitaxel and vinblastine at low doses can increase immune priming by stimulating the maturation and activation of dendritic antigen-presenting cells [49,50]. Microtubule-targeting agents also stimulate the T-cell response against tumors. For example, docetaxel treatment increases the $T_{eff}/T_{reg}$ ratio [51] and neoadjuvant paclitaxel

treatment increases tumor-infiltrating lymphocytes in patients with breast cancer [52]. Together, this evidence provides strong support for further development of DZ-2384 for the treatment of metastatic TNBC as a single agent or in addition to immune checkpoint inhibitors.

## Acknowledgements

The authors thank the patients who provided tissue, the MUHC breast surgeons, and the pathologists.

This research was funded by Diazon Pharmaceuticals to G.C.S. M.D. is funded by the McGill MD/PhD program and the Brain Tumor Foundation of Canada. P.S. is a Vanier Scholar. M.P. holds the Diane and Sal Guerrera Chair in Cancer Genetics at McGill University and is supported by the Reseau de Recherche en Cancer of the FRQS (FRQ-34787), CIHR (FDN-143281) and SU2C (SU2C-AACR-DT-1815).

### Conflicts of interest

A.R. and G.C.S. are co-founders of Diazon Pharmaceuticals. For the remaining authors, there are no conflicts of interest.

## References

1 Carey LA, Dees EC, Sawyer L, Gatti L, Moore DT, Collichio F, *et al*. The triple negative paradox: primary tumor chemosensitivity of breast cancer subtypes. *Clin Cancer Res* 2007; **13**:2329–2334.
2 Lehmann BD, Pietenpol JA. Clinical implications of molecular heterogeneity in triple negative breast cancer. *Breast* 2015; **24** (**Suppl 2**):S36–S40.
3 O'Reilly EA, Gubbins L, Sharma S, Tully R, Guang MH, Weiner-Gorzel K, *et al*. The fate of chemoresistance in triple negative breast cancer (TNBC). *BBA Clin* 2015; **3**:257–275.
4 Hudis CA, Gianni L. Triple-negative breast cancer: an unmet medical need. *Oncologist* 2011; **16** (**Suppl 1**):1–11.
5 Pogoda K, Niwinska A, Murawska M, Pienkowski T. Analysis of pattern, time and risk factors influencing recurrence in triple-negative breast cancer patients. *Med Oncol* 2013; **30**:388.
6 Rowinsky EK. The development and clinical utility of the taxane class of antimicrotubule chemotherapy agents. *Annu Rev Med* 1997; **48**:353–374.
7 Bracci L, Schiavoni G, Sistigu A, Belardelli F. Immune-based mechanisms of cytotoxic chemotherapy: implications for the design of novel and rationale-based combined treatments against cancer. *Cell Death Differ* 2014; **21**:15–25.
8 Dushyanthen S, Beavis PA, Savas P, Teo ZL, Zhou C, Mansour M, *et al*. Relevance of tumor-infiltrating lymphocytes in breast cancer. *BMC Med* 2015; **13**:202.
9 Saleh SMI, Bertos N, Gruosso T, Gigoux M, Souleimanova M, Zhao H, *et al*. Identification of interacting stromal axes in triple-negative breast cancer. *Cancer Res* 2017; **77**:4673–4683.
10 Nanda R, Chow LQ, Dees EC, Berger R, Gupta S, Geva R, *et al*. Pembrolizumab in patients with advanced triple-negative breast cancer: phase Ib KEYNOTE-012 Study. *J Clin Oncol* 2016; **34**:2460–2467.
11 Cha E, Wallin J, Kowanetz M. PD-L1 inhibition with MPDL3280A for solid tumors. *Semin Oncol* 2015; **42**:484–487.
12 Herbst RS, Soria JC, Kowanetz M, Fine GD, Hamid O, Gordon MS, *et al*. Predictive correlates of response to the anti-PD-L1 antibody MPDL3280A in cancer patients. *Nature* 2014; **515**:563–567.
13 Nanda R, Liu M, Yau C, Asare S, Hylton N, Van't Veer L, *et al*. Pembrolizumab plus standard neoadjuvant therapy for high-risk breast cancer (BC): results from I-SPY-2. *J Clin Oncol* 2017; **35** (**Suppl**):506.
14 Lindquist N, Fenical W, Van Duyne GD, Clardy J. Isolation and structure determination of diazonamides A and B, unusual cytotoxic metabolites from the marine ascidian Diazona chinensis. *J Am Chem Soc* 1991; **113**:2303–2304.
15 Li J, Burgett AW, Esser L, Amezcua C, Harran PG. Total synthesis of nominal diazonamides-part 2: on the true structure and origin of natural isolates. *Angew Chem Int Ed Engl* 2001; **40**:4770–4773.
16 Williams NS, Burgett AW, Atkins AS, Wang X, Harran PG, McKnight SL. Therapeutic anticancer efficacy of a synthetic diazonamide analog in the absence of overt toxicity. *Proc Natl Acad Sci USA* 2007; **104**:2074–2079.
17 Wieczorek M, Tcherkezian J, Bernier C, Prota AE, Chaaban S, Rolland Y, *et al*. The synthetic diazonamide DZ-2384 has distinct effects on microtubule curvature and dynamics without neurotoxicity. *Sci Transl Med* 2016; **8**:365ra159.
18 Ding H, DeRoy PL, Perreault C, Larivée A, Siddiqui A, Caldwell CG, *et al*. Electrolytic macrocyclizations: scalable synthesis of a diazonamide-based drug development candidate. *Angew Chem Int Ed Engl* 2015; **54**:4818–4822.
19 Minn AJ, Gupta GP, Siegel PM, Bos PD, Shu W, Giri DD, *et al*. Genes that mediate breast cancer metastasis to lung. *Nature* 2005; **436**:518–524.
20 Bos PD, Zhang XH, Nadal C, Shu W, Gomis RR, Nguyen DX, *et al*. Genes that mediate breast cancer metastasis to the brain. *Nature* 2009; **459**:1005–1009.
21 Donoghue JF, Bogler O, Johns TG. A simple guide screw method for intracranial xenograft studies in mice. *J Vis Exp* 2011; **(55)**:3157.
22 Leccia F, Del Vecchio L, Mariotti E, Di Noto R, Morel AP, Puisieux A, *et al*. ABCG2, a novel antigen to sort luminal progenitors of BRCA1-breast cancer cells. *Mol Cancer* 2014; **13**:213.
23 Liu Y, Du F, Chen W, Yao M, Lv K, Fu P. EIF5A2 is a novel chemoresistance gene in breast cancer. *Breast Cancer* 2015; **22**:602–607.
24 Gilabert M, Launay S, Ginestier C, Bertucci F, Audebert S, Pophillat M, *et al*. Poly(ADP-ribose) polymerase 1 (PARP1) overexpression in human breast cancer stem cells and resistance to olaparib. *PLoS One* 2014; **9**:e104302.
25 Dobrolecki LE, Airhart SD, Alferez DG, Aparicio S, Behbod F, Bentires-Alj M, *et al*. Patient-derived xenograft (PDX) models in basic and translational breast cancer research. *Cancer Metastasis Rev* 2016; **35**:547–573.
26 Wei S, Siegal GP. Metastatic organotropism: an intrinsic property of breast cancer molecular subtypes. *Adv Anat Pathol* 2017; **24**:78–81.
27 Kennecke H, Yerushalmi R, Woods R, Cheang MC, Voduc D, Speers CH, *et al*. Metastatic behavior of breast cancer subtypes. *J Clin Oncol* 2010; **28**:3271–3277.
28 Lin NU, Claus E, Sohl J, Razzak AR, Arnaout A, Winer EP. Sites of distant recurrence and clinical outcomes in patients with metastatic triple-negative breast cancer: high incidence of central nervous system metastases. *Cancer* 2008; **113**:2638–2645.
29 Witzel I, Oliveira-Ferrer L, Pantel K, Muller V, Wikman H. Breast cancer brain metastases: biology and new clinical perspectives. *Breast Cancer Res* 2016; **18**:8.
30 Gianni L, Kearns CM, Giani A, Capri G, Vigano L, Lacatelli A, *et al*. Nonlinear pharmacokinetics and metabolism of paclitaxel and its pharmacokinetic/pharmacodynamic relationships in humans. *J Clin Oncol* 1995; **13**:180–190.
31 Bruno R, Hille D, Riva A, Vivier N, ten Bokkel Huinnink WW, van Oosterom AT, *et al*. Population pharmacokinetics/pharmacodynamics of docetaxel in phase II studies in patients with cancer. *J Clin Oncol* 1998; **16**:187–196.
32 Clarke SJ, Rivory LP. Clinical pharmacokinetics of docetaxel. *Clin Pharmacokinet* 1999; **36**:99–114.
33 Hendrikx JJ, Lagas JS, Wagenaar E, Rosing H, Schellens JH, Beijnen JH, *et al*. Oral co-administration of elacridar and ritonavir enhances plasma levels of oral paclitaxel and docetaxel without affecting relative brain accumulation. *Br J Cancer* 2014; **110**:2669–2676.
34 Kemper EM, van Zandbergen AE, Cleypool C, Mos HA, Boogerd W, Beijnen JH, *et al*. Increased penetration of paclitaxel into the brain by inhibition of P-glycoprotein. *Clin Cancer Res* 2003; **9**:2849–2855.
35 Motoshima T, Komohara Y, Horlad H, Takeuchi A, Maeda Y, Tanoue K, *et al*. Sorafenib enhances the antitumor effects of anti-CTLA-4 antibody in a murine cancer model by inhibiting myeloid-derived suppressor cells. *Oncol Rep* 2015; **33**:2947–2953.
36 Proietti E, Moschella F, Capone I, Belardelli F. Exploitation of the propulsive force of chemotherapy for improving the response to cancer immunotherapy. *Mol Oncol* 2012; **6**:1–14.
37 Steeg PS, Camphausen KA, Smith QR. Brain metastases as preventive and therapeutic targets. *Nat Rev Cancer* 2011; **11**:352–363.
38 Fidler IJ. The role of the organ microenvironment in brain metastasis. *Semin Cancer Biol* 2011; **21**:107–112.
39 Parks SK, Chiche J, Pouyssegur J. Disrupting proton dynamics and energy metabolism for cancer therapy. *Nat Rev Cancer* 2013; **13**:611–623.
40 Mahoney BP, Raghunand N, Baggett B, Gillies RJ. Tumor acidity, ion trapping and chemotherapeutics. I. Acid pH affects the distribution of chemotherapeutic agents in vitro. *Biochem Pharmacol* 2003; **66**:1207–1218.

41 Tunggal JK, Melo T, Ballinger JR, Tannock IF. The influence of expression of P-glycoprotein on the penetration of anticancer drugs through multicellular layers. *Int J Cancer* 2000; **86**:101–107.
42 Coley HM, Amos WB, Twentyman PR, Workman P. Examination by laser scanning confocal fluorescence imaging microscopy of the subcellular localisation of anthracyclines in parent and multidrug resistant cell lines. *Br J Cancer* 1993; **67**:1316–1323.
43 Galluzzi L, Buque A, Kepp O, Zitvogel L, Kroemer G. Immunological effects of conventional chemotherapy and targeted anticancer agents. *Cancer Cell* 2015; **28**:690–714.
44 Cimino-Mathews A, Thompson E, Taube JM, Ye X, Lu Y, Meeker A, *et al*. PD-L1 (B7-H1) expression and the immune tumor microenvironment in primary and metastatic breast carcinomas. *Hum Pathol* 2016; **47**:52–63.
45 Li X, Li M, Lian Z, Zhu H, Kong L, Wang P, *et al*. Prognostic role of programmed death ligand-1 expression in breast cancer: a systematic review and meta-analysis. *Target Oncol* 2016; **11**:753–761.
46 Dua I, Tan AR. Immunotherapy for triple-negative breast cancer: a focus on immune checkpoint inhibitors. *Am J Hematol-Oncol* 2017; **13**:20–27.
47 Javeed A, Ashraf M, Riaz A, Ghafoor A, Afzal S, Mukhtar MM. Paclitaxel and immune system. *Eur J Pharm Sci* 2009; **38**:283–290.
48 Kim JY, Lee E, Park K, Park WY, Jung HH, Ahn JS, *et al*. Immune signature of metastatic breast cancer: identifying predictive markers of immunotherapy response. *Oncotarget* 2017; **8**:47400–47411.
49 Emens LA, Jaffee EM. Leveraging the activity of tumor vaccines with cytotoxic chemotherapy. *Cancer Res* 2005; **65**:8059–8064.
50 Tanaka H, Matsushima H, Nishibu A, Clausen BE, Takashima A. Dual therapeutic efficacy of vinblastine as a unique chemotherapeutic agent capable of inducing dendritic cell maturation. *Cancer Res* 2009; **69**:6987–6994.
51 Roselli M, Cereda V, di Bari MG, Formica V, Spila A, Jochems C, *et al*. Effects of conventional therapeutic interventions on the number and function of regulatory T cells. *Oncoimmunology* 2013; **2**:e27025.
52 Demaria S, Volm MD, Shapiro RL, Yee HT, Oratz R, Formenti SC, *et al*. Development of tumor-infiltrating lymphocytes in breast cancer after neoadjuvant paclitaxel chemotherapy. *Clin Cancer Res* 2001; **7**:3025–3030.